

On the Distribution of the Sum of Málaga- \mathcal{M} Random Variables and Applications

Elmehdi Illi, *Member, IEEE*, Faissal El Bouanani, *Senior Member, IEEE*, and Fouad Ayoub, *Member, IEEE*

Abstract—In this paper, a very accurate approximation method for the statistics of the sum of Málaga- \mathcal{M} random variates with pointing error (MRVs) is proposed. In particular, the probability density function of MRV is approximated by a Fox's H -function through the moment-based approach. Then, the respective moment-generating function of the sum of N MRVs is provided, based on which the average symbol error rate is evaluated for an N -branch maximal-ratio combining (MRC) receiver. The retrieved results show that the proposed approximate results match accurately with the exact simulated ones. Additionally, the results show that the achievable diversity order increases as a function of the number of MRC diversity branches.

Index Terms—Average symbol error rate, free-space optics, Málaga- \mathcal{M} distribution, moment-generating function, probability density function, sum of random variates.

I. INTRODUCTION

In recent years, there has been an increasing interest in deriving the statistical properties of the sum of random variates (RVs), namely the probability density function (PDF) and the moment-generating function (MGF). Such statistical properties are of paramount importance in analyzing the performance of wireless communication systems (WCSs) employing multiple-input multiple-output (MIMO) schemes and maximal-ratio combining (MRC) diversity technique.

Málaga- \mathcal{M} distribution has been widely advocated as a universal model for representing the atmospheric turbulence impairment in free-space optical (FSO) links [1], [2], as it generalizes several turbulence-induced fading models (e.g., shadowed-Rician, Gamma-Gamma, Log-Normal, double Weibull) [2]. From another front, there has been a rising attention in the analysis of MIMO FSO WCSs employing MRC combining scheme, where the output SNR is the sum of the SNRs on the receiver branches. For instance, the authors in [3] dealt with the capacity performance of a multiple-input single-output (MISO) FSO system employing equal-gain combining technique, subject to Gamma-Gamma fading and pointing error impairment (PEI). Additionally, the authors in [4] dealt with the outage and average bit error rate performance for both MRC and selection combining techniques over Gamma-Gamma fading. Importantly, the work in [5] analyzed the performance of an M -branch MISO FSO system using maximal-ratio transmission, where the FSO links undergo Málaga- \mathcal{M} fading without PEI.

On the other hand, other works such as [6], [7] dealt with the distribution of the product of shadowed-Rician RVs.

From the above-mentioned works, the authors assessed the performance of FSO systems employing either MRC or EGC receivers, subject to either Gamma-Gamma with PEI or Málaga- \mathcal{M} fading model without PEI. To the best of the authors' knowledge, neither the sum of Málaga- \mathcal{M} RVs with PEI (MRVs) nor the analytical performance of FSO system employing MRC receiver, subject to Málaga- \mathcal{M} fading with PEI have been investigated before in the literature. Throughout this paper, and distinctly from the works [3], [5], [8], we aim at proposing a highly-accurate approximation for the statistics of the sum of MRVs. In particular, we approximate the PDF of MRV through a Meijer's G -function, by the use of the moments-based approach. Distinct from [9], the first six moments of the distribution are evaluated instead of only the first five ones, so as to enhance the approximation accuracy. Capitalizing on this result, the MGF of the sum of MRVs is retrieved, based on which the respective average symbol error rate (ASER) for a single-input multiple-output (SIMO) FSO system employing MRC scheme is evaluated in approximate and asymptotic forms. The derived MGF and ASER results are provided for two cases: (i) independent and identically-distributed (i.i.d), and (ii) independent and non-identically distributed (i.n.i.d) MRVs. Importantly, the derived results are generalizing the ones of an FSO system employing MRC receiver, subject either to traditional Málaga- \mathcal{M} fading model without PEI, investigated in [5], or subject to Gamma-Gamma fading model with PEI, inspected in [3], [8].

The main contributions of this work are given as follows: First, we propose an accurate approximate expression of the MRV's PDF. Then, we retrieve the MGF of the sum of MRVs for both i.i.d and i.n.i.d cases. Based on these last-mentioned results, we derive the ASER and its asymptotic expressions for various modulations of an N -branch MRC receiver in approximate form, for both aforementioned cases. It is further demonstrated that the achievable diversity order is increasing with the increase in the number of MRC branches.

II. PROPOSED APPROXIMATION

In this section, a simple and accurate approximate PDF for the MRV is presented, based on which the MGF of the sum of MRVs is derived, for both i.i.d and i.n.i.d cases.

E. Illi and F. El Bouanani are with ENSIAS College of Engineering, Mohammed V University, Rabat, Morocco (e-mails: {elmehdi.illi, f.elbouanani}@um5s.net.ma).

F. Ayoub is with CRMEF, Kenitra, Morocco (e-mail: ayoub@crmefk.ma).

A. Probability Density Function

Let γ be an MRV encompassing the atmospheric turbulence and the PEI with PDF [1]¹

$$f_\gamma(x) = \frac{\xi^2 A}{2x} \sum_{m=1}^{\beta} b_m G_{1,3}^{3,0} \left(\frac{Bx}{\mu_1} \middle| \begin{matrix} -; \xi^2 + 1 \\ \xi^2, \alpha, m; - \end{matrix} \right), x > 0; \quad (1)$$

where $A = \frac{2\alpha^{\frac{\alpha}{2}}}{h_j^{1+\frac{\alpha}{2}} \Gamma(\alpha)} \left(\frac{\beta}{\beta + \frac{\Omega'}{h}} \right)^{\beta + \frac{\alpha}{2}}$, α and β are the atmospheric turbulence severity parameters, $h = 2d_o(1 - \epsilon)$ and $\Omega' = \Omega + 2d_o\epsilon + 2\sqrt{2d_o\epsilon\Omega} \cos(\Theta_A - \Theta_B)$ denote the average power of the scattering component received by off-axis eddies and the one of the coherent contributions, respectively, with $2d_o$ is the average power of the total scatter components, ϵ is the amount of scattering power coupled-to-LOS component, Ω is the average power of the dominant LOS component, and Θ_A and Θ_B are deterministic phases of the LOS and coupled-to-LOS terms, respectively. Besides, $G_{p,q}^{m,n}(\cdot|\cdot)$ refers to the Meijer's G -function [10], $B = \frac{\xi^2 \alpha \beta (h + \Omega')}{(\xi^2 + 1)(h\beta + \Omega')}$, ξ denotes the PEI severity parameter, and $\mu_1 = \mathbb{E}[\gamma]$ stands for the average value of γ , where $\mathbb{E}[\cdot]$ refers to the expectation operator [11]. Furthermore, $b_m = \frac{(\beta-1)}{(m-1)} \frac{(h\beta + \Omega')^{1+\frac{\alpha}{2}}}{(m-1)!} \left(\frac{\Omega'}{h} \right)^{m-1} \beta^{-\frac{\alpha}{2}-m} \alpha^{-\frac{\alpha}{2}}$.

Proposition 1. *The PDF of γ can be approximated accurately as follows*

$$f_\gamma(x) \approx a_1 G_{2,2}^{2,0} \left(\frac{x}{a_2} \middle| \begin{matrix} -; a_3, a_4 \\ a_5, a_6; - \end{matrix} \right), \quad (2)$$

where

$$a_1 = \frac{\Gamma(a_3 + 1) \Gamma(a_4 + 1)}{a_2 \Gamma(a_5 + 1) \Gamma(a_6 + 1)}, \quad (3)$$

$$a_2 = \frac{\mathcal{L}_4}{2} - \mathcal{L}_3 + \frac{\mathcal{L}_2}{2}, \quad (4)$$

$$a_3 = \frac{-4\mathcal{G}_4 + 9\mathcal{G}_3 - 6\mathcal{G}_2 + \mathcal{G}_1}{\mathcal{G}_4 - 3\mathcal{G}_3 + 3\mathcal{G}_2 - \mathcal{G}_1}, \quad (5)$$

$$a_4 = \frac{-\phi - \sqrt{\phi^2 - 4(\delta p + \lambda r)(\lambda q + \sigma s)}}{2(\delta p + \lambda r)}, \quad (6)$$

$$a_5 = \frac{\kappa - \sqrt{\kappa^2 - 4\eta}}{2} - 1, \quad (7)$$

$$a_6 = \frac{\kappa + \sqrt{\kappa^2 - 4\eta}}{2} - 1, \quad (8)$$

with

$$\mathcal{L}_i = \varphi_i (a_4 + i) (a_3 + i), \quad (9)$$

$$\mathcal{G}_i = \varphi_i (a_4 + i), \quad (10)$$

$$\phi = \lambda(p + s) + \sigma r + \delta q, \quad (11)$$

$$\lambda = 5\varphi_5 - 12\varphi_4 + 9\varphi_3 - 2\varphi_2, \quad (12)$$

$$p = -4\varphi_4 + 9\varphi_3 - 6\varphi_2 + \mu_1, \quad (13)$$

$$s = 4\varphi_4 - 9\varphi_3 + 6\varphi_2 - \mu_1, \quad (14)$$

$$\sigma = 25\varphi_5 - 48\varphi_4 + 27\varphi_3 - 4\varphi_2, \quad (15)$$

$$r = \varphi_4 - 3\varphi_3 + 3\varphi_2 - \mu_1, \quad (16)$$

$$\delta = \varphi_5 - 3\varphi_4 + 3\varphi_3 - \varphi_2, \quad (17)$$

$$q = \mu_1 - 16\varphi_4 + 27\varphi_3 - 12\varphi_2, \quad (18)$$

$$\kappa = \frac{\mathcal{L}_2 - \mathcal{L}_1}{a_2} - 1, \quad (19)$$

$$\eta = \frac{\mathcal{L}_1}{a_2}, \quad (20)$$

and $\varphi_i = \frac{\mu_i}{\mu_{i-1}}$ ($i \geq 1$), μ_i is the i -th moment of γ , and $\Gamma(\cdot)$ is the Gamma function [12, Eq. (8.350.1)].

Remark 1. *Interestingly, such approximation with all the above parameters remains accurate for other kinds of distributions.*

Proof: The proof is provided in Appendix A. ■

Remark 2. *First, it is clearly seen that μ_i is proportional to μ_1^i . It follows that φ_i , and consequently the parameters defined in (12)-(17), are proportional to μ_1 , while ϕ is proportional to μ_1^2 . Thus, a_4 , given in (6), is unitless. Therefore, it yields from (5) and (10) that a_3 is also unitless. Furthermore, one can notice also from (4) and (9) that a_2 is proportional to μ_1 , and that κ and η are unitless. Lastly, a_5 and a_6 are then unitless, and a_1 is inversely proportional to μ_1 .*

B. Moment-Generating Function

Corollary 1. *The MGF of γ can be approximated as follows*

$$M_\gamma(s) \approx \frac{a_1}{s} G_{3,2}^{2,1} \left(\frac{1}{sa_2} \middle| \begin{matrix} 0; a_3, a_4 \\ a_5, a_6; - \end{matrix} \right); s > 0. \quad (21)$$

Proof: The MGF of γ can be evaluated as follows

$$M_\gamma(s) = \int_0^\infty e^{-sx} f_\gamma(x) dx. \quad (22)$$

By plugging (2) into (22), and making use of the Laplace transform [13, Eq. (2.19)], (21) is reached. ■

Proposition 2. *Let us consider the set $\{\gamma_j\}_{1 \leq j \leq N}$ of MRVs with parameters $\alpha^{(j)}$, $\beta^{(j)}$, $\xi^{(j)}$, and $\mu_1^{(j)}$. The MGF of $\gamma_T = \sum_{j=1}^N \gamma_j$ can be expressed in an approximate form as*

$$M_{\gamma_T}^{(i.i.d)}(s) \approx N! \left(\frac{a_1}{s} \right)^N \sum_{k_1+k_2=N} \frac{(k_1!k_2!)^{-1}}{a_2^{\mathcal{K}_{k_1,k_2}}} \times \sum_{l=0}^{\infty} \sum_{q_1+q_2=l} c_{q_1}^{(1)} c_{q_2}^{(2)} s^{-ql, k_1, k_2}, \quad (23)$$

and

$$M_{\gamma_T}^{(i.n.i.d)}(s) \approx \sum_{\substack{k_1+k_2+\dots+k_N \geq N \\ k_j=1,2}} \prod_{j=1}^N \left(a_{1,j} a_{2,j}^{-a_{k_j+4,j}} \right) \times \sum_{l=0}^{\infty} s^{-v-N-l} \sum_{q_1+q_2+\dots+q_N=l} \prod_{i=1}^N b_{q_i}^{(k_i)}, \quad (24)$$

¹We consider in this work the Málaga- \mathcal{M} distribution as in [1] for the case of coherent heterodyne detection (i.e., $r = 1$).

for i.i.d and i.n.i.d cases, respectively, where $\varkappa_{k_1, k_2} = a_5 k_1 + a_6 k_2$, $\varrho_{l, k_1, k_2} = \varkappa_{k_1, k_2} + l$, $v = \sum_{j=1}^N a_{k_j+4, j}$,

$$c_m^{(i)} = \begin{cases} \left(b_0^{(i)}\right)^{k_i}, m = 0 \\ \frac{1}{m b_0^{(i)}} \sum_{l=1}^m (lk_i - m + l) b_l^{(i)} c_{m-l}^{(i)}; m \geq 1 \end{cases}, \quad (25)$$

and

$$b_l^{(i)} = \frac{(-1)^l \Gamma(1 + a_{i+4} + l) \Gamma((3 - 2i)(a_6 - a_5) - l)}{l! \Gamma(a_3 - a_{i+4} - l) \Gamma(a_4 - a_{i+4} - l) a_2^l}. \quad (26)$$

Remark 3. $a_{i,j}$ and $b_{l,j}^{(k)}$ represent the coefficients a_i and $b_l^{(k)}$ for the i.n.i.d case, respectively with $j = 1, \dots, N$.

Proof: The MGF in (21) can be written through the Mellin-Barnes definition as [13, Eq. (1.112)]

$$M_{\gamma_j}(s) \approx \frac{a_{1,j}}{2\pi i s} \int_{C_t} \frac{\Gamma(a_{5,j} + t) \Gamma(a_{6,j} + t) \Gamma(1 - t)}{\Gamma(a_{3,j} + t) \Gamma(a_{4,j} + t) (sa_{2,j})^{-t}} dt, \quad (27)$$

where $i^2 = -1$. Using the residues theorem [10, Theorem 1.2], the MGF in (27) can be written as the summation of the residues evaluated at the left poles of the associated integrand function as [10, Eqs. (1.3.5), (1.3.6)]

$$M_{\gamma_j}(s) = \frac{a_{1,j} (\Delta_{1,j} + \Delta_{2,j})}{s}, \quad (28)$$

with

$$\Delta_{k,j} = (sa_{2,j})^{-a_{k+4,j}} \sum_{l=0}^{\infty} b_{l,j}^{(k)} s^{-l}; k = 1, 2, \quad (29)$$

and $b_{l,j}^{(k)}$ being defined similarly to $b_l^{(k)}$ in (3) by replacing a_i by $a_{i,j}$. On the other hand, since $\gamma_T = \sum_{j=1}^N \gamma_j$, the MGF of γ_T is expressed as

$$M_{\gamma_T}^{(i.i.d)}(s) = [M_{\gamma_j}(s)]^N, \quad (30)$$

$$M_{\gamma_T}^{(i.n.i.d)}(s) = \prod_{j=1}^N M_{\gamma_j}(s), \quad (31)$$

for the i.i.d and i.n.i.d cases, respectively. Furthermore, by assuming $a_{i,j} = a_i$ and $b_{l,j}^{(k)} = b_l^{(k)}$ for the i.i.d case, and using the multinomial theorem as well as [12, Eq. (0.314)] alongside with some algebraic manipulations, (23) is attained. Finally, by rearranging the products of $\Delta_{k,j}$ ($k = 1, 2, j = 1, \dots, N$) and retrieving the scale factors of s^{-l} , (24) is obtained. ■

III. ERROR RATE ANALYSIS

In this section, and capitalizing on the previously derived results, the ASER of a SIMO FSO-based WCS, employing MRC technique, is inspected. In the considered system, an optical transmitter, consisting of a LED/Laser, transmits an optical beam through a turbulent channel toward a receiver equipped by several optical apertures. In particular, the ASER of the considered WCS, for various coherent modulations is inspected under both i.i.d and i.n.i.d cases. Also, asymptotic representations of this metric over both cases are derived.

A. Approximate Analysis

Proposition 3. The ASER for various modulations and N -branch MRC receiver, subject to Málaga- \mathcal{M} turbulence-induced fading with PEI, can be approximated as

$$\begin{aligned} \overline{P}_s^{(i.i.d)} &\approx \frac{\rho}{\pi} \left(\frac{4a_1}{\theta}\right)^N \sum_{k_1+k_2=N} \frac{N! (\theta a_2)^{-\varkappa_{k_1, k_2}}}{k_1! k_2!} \\ &\times \sum_{l=0}^{\infty} \sum_{q_1+q_2=l} c_{q_1}^{(1)} c_{q_2}^{(2)} \theta^{-l} 4^{\varrho_{l, k_1, k_2}} \\ &\times \mathcal{B}\left(N + \varrho_{l, k_1, k_2} + \frac{1}{2}, N + \varrho_{l, k_1, k_2} + \frac{1}{2}\right), \quad (32) \end{aligned}$$

and

$$\begin{aligned} \overline{P}_s^{(i.n.i.d)} &\approx \frac{\rho}{\pi} \sum_{\substack{k_1+k_2+\dots+k_N \geq N \\ k_j=1,2}} \prod_{j=1}^N \left(a_{1,j} a_{2,j}^{-a_{k_j+4,j}}\right) \\ &\times \sum_{l=0}^{\infty} \mathcal{B}\left(v + N + l + \frac{1}{2}, v + N + l + \frac{1}{2}\right) \\ &\times \left(\frac{4}{\theta}\right)^{v+N+l} \sum_{q_1+q_2+\dots+q_N=l} \prod_{j=1}^N b_{q_j,j}^{(k_j)}, \quad (33) \end{aligned}$$

for the i.i.d and i.n.i.d cases, respectively, where ρ and θ are modulation-dependent parameters, and $\mathcal{B}(\cdot, \cdot)$ refers to the beta function [12, Eq. (8.384.1)].

Proof: The ASER can be expressed using the MGF as [11, Eq. (23)]

$$\overline{P}_s^{(x)} = \frac{2\rho}{\pi} \int_0^{\frac{\pi}{2}} M_{\gamma_T}^{(x)} \left(\frac{\theta}{\sin^2 \phi}\right) d\phi, \quad (34)$$

with $x \in \{i.i.d, i.n.i.d\}$. By plugging (23)-(24) into (34), it yields

$$\begin{aligned} \overline{P}_s^{(i.i.d)} &\approx \frac{2\rho}{\pi} N! \left(\frac{a_1}{s}\right)^N \sum_{k_1+k_2=N} \frac{(k_1! k_2!)^{-1}}{a_2^{\varkappa_{k_1, k_2}}} \\ &\times \sum_{l=0}^{\infty} \sum_{q_1+q_2=l} \frac{c_{q_1}^{(1)} c_{q_2}^{(2)}}{\theta^{\varrho_{l, k_1, k_2}}} \int_0^{\frac{\pi}{2}} (\sin \phi)^{2\varrho_{l, k_1, k_2}} d\phi, \quad (35) \end{aligned}$$

and

$$\begin{aligned} \overline{P}_s^{(i.n.i.d)} &\approx \frac{2\rho}{\pi} \sum_{\substack{k_1+k_2+\dots+k_N \geq N \\ k_j=1,2}} \prod_{j=1}^N \left(a_{1,j} a_{2,j}^{-a_{k_j+4,j}}\right) \sum_{l=0}^{\infty} \theta^{-v-N-l} \\ &\times \int_0^{\frac{\pi}{2}} (\sin^2 \phi)^{2(v+N+l)} d\phi \sum_{q_1+q_2+\dots+q_N=l} \prod_{i=1}^N b_{q_i,i}^{(k_i)}. \quad (36) \end{aligned}$$

Lastly, by using [12, Eq. (3.621.1)], (32)-(33) are reached. ■

Remark 4. For Málaga- \mathcal{M} distribution with PEI, μ_1 or $\mu_1^{(j)}$ represents the average electrical SNR per receiver's branch. Importantly, from **Remark 2**, the higher μ_1 and $\mu_1^{(j)}$ are, the lower are a_1 and $a_{1,j}$ and the greater are a_2 and $a_{2,j}$, respectively. Therefore, it can be seen that the MGF and ASER of the considered system, given in (23), (24), (32), and (33) are decreasing with respect to μ_1 and $\mu_1^{(j)}$.

B. Asymptotic Analysis

Corollary 2. In the high SNR regime (i.e., $\mu_1 \rightarrow \infty$), the ASER can be asymptotically approximated, for both i.i.d and i.n.i.d cases, as follows

$$\bar{P}_s^{(i.i.d,\infty)} \sim G_c^{(i.i.d)} a_2^{-G_d^{(i.i.d)}}, \quad (37)$$

$$\begin{aligned} \bar{P}_s^{(i.n.i.d,\infty)} &\sim \frac{\rho}{\pi} \mathcal{B}\left(\zeta + N + \frac{1}{2}, \zeta + N + \frac{1}{2}\right) \\ &\times \left(\frac{4}{\theta}\right)^{\zeta+N} \prod_{j=1}^N \left(b_{0,j}^{(g_j)} \tau^{(j)} a_{2,j}^{-a_{g_j+4,j-1}}\right), \end{aligned} \quad (38)$$

where the coding gain and achievable diversity order for the i.i.d case are

$$\begin{aligned} G_c^{(i.i.d)} &= \frac{\rho}{\pi} \left(\left(\frac{4}{\theta}\right)^{a_{m+4}+1} \tau b_0^{(m)}\right)^N \\ &\times \mathcal{B}\left(N(a_{m+4}+1) + \frac{1}{2}, N(a_{m+4}+1) + \frac{1}{2}\right), \end{aligned} \quad (39)$$

and

$$G_d^{(i.i.d)} = N(a_{m+4}+1), \quad (40)$$

respectively, with $\tau = \frac{\Gamma(a_3+1)\Gamma(a_4+1)}{\Gamma(a_5+1)\Gamma(a_6+1)}$, $m = \begin{cases} 1, & a_5 < a_6 \\ 2, & a_5 > a_6 \end{cases}$, $\zeta = \sum_{j=1}^N a_{g_j+4,j}$, and $a_{g_j+4,j} = \min(a_{5,j}, a_{6,j})$.

Proof: When $\mu_1^{(j)} \rightarrow \infty$, it yields from Remark 2 that $a_{1,j}$ and $a_{2,j}$ goes to zero and infinity, respectively. Therefore, the ASER for the i.i.d case, given in (32), can be expanded by the least power of $1/a_2$. Thus, from (25)-(26), it is evident that $c_{q_i}^{(i)}$ is inversely proportional to $a_2^{q_i}$. Therefore, only the first term of the infinite summation is considered, i.e., $q_1 = q_2 = l = 0$. Hence, by plugging (3) and (25) with $m = 0$ into (32), it yields

$$\begin{aligned} \bar{P}_s^{(i.i.d,\infty)} &\sim \frac{\rho}{\pi} \left(\frac{4\tau}{\theta a_2}\right)^N \sum_{k_1+k_2=N} \frac{N!}{k_1!k_2!} \left(\frac{4}{\theta a_2}\right)^{\varkappa_{k_1,k_2}} \left(b_0^{(1)}\right)^{k_1} \\ &\times \left(b_0^{(2)}\right)^{k_2} \mathcal{B}\left(N + \varkappa_{k_1,k_2} + \frac{1}{2}, N + \varkappa_{k_1,k_2} + \frac{1}{2}\right). \end{aligned} \quad (41)$$

In (41), only the least power of $1/a_2$ is kept, i.e., $\min(\varkappa_{k_1,k_2}) + N$. As $k_2 = N - k_1$, it yields that $\varkappa_{k_1,k_2} = \varrho_{k_1} = k_1(a_5 - a_6) + Na_6$, which its monotony depends on the sign of $a_5 - a_6$. As a result, its minimum corresponds to $k_1 = 0$ (i.e., $k_2 = N$) if $a_5 > a_6$, or $k_1 = N$ (i.e., $k_2 = 0$) otherwise. Consequently, it yields $\min(\varrho_{k_1}) = N \min(a_5, a_6)$. Lastly, by keeping only the two aforementioned values of the pair (k_1, k_2) on the multinomial summation in (41), we obtain (37).

² τ is denoted $\tau^{(j)}$ for the i.n.i.d case.

Analogously, and by taking only the first terms $b_{0,i}^{(k_i)}$ (i.e., $q_1 = q_2 = \dots = q_N = l = 0$), and using (3), the ASER in (33) can be expanded as

$$\begin{aligned} \bar{P}_s^{(i.n.i.d,\infty)} &\sim \frac{\rho}{\pi} \sum_{\substack{k_1+k_2+\dots+k_N \geq N \\ k_j=1,2}} \prod_{j=1}^N \left(\tau^{(j)} a_{2,j}^{-a_{k_j+4,j-1}}\right) \\ &\times \left(\frac{4}{\theta}\right)^{v+N} \mathcal{B}\left(v + N + \frac{1}{2}, v + N + \frac{1}{2}\right) \prod_{j=1}^N b_{0,j}^{(k_j)}. \end{aligned} \quad (42)$$

Thus, only the terms $a_{2,j}$ with least powers are kept. Therefore, we define the indices g_j satisfying $a_{g_j+4,j} = \min(a_{5,j}, a_{6,j})$, which yields the least powers of $a_{2,j}$. Consequently, by substituting k_j by g_j and v by $\zeta = \sum_{j=1}^N a_{g_j+4,j}$, (38) is achieved. ■

Remark 5. From [1, Eq. (20)], one can see that μ_i is a function of α , β , and ξ^2 , which yields that φ_i depends on the same parameters. Consequently, it yields from (7), (8), (9), (19), and (20) that a_5 and a_6 depend also on α , β , and ξ^2 . As a result, it yields from (40) that the system's achievable diversity order for the i.i.d case depends only on the number of branches N and the turbulence and PEI severity parameters (i.e., α , β , and ξ^2).

IV. NUMERICAL RESULTS

In this section, some representative numerical examples are depicted in order to highlight the effects of the key system parameters on the derived PDF, MGFs, and ASER for both i.i.d and i.n.i.d cases. To this end, we set the parameters $\alpha^{(j)} = 2.296$ (Except Fig. 6), $\beta^{(j)} = 2$ (Except Fig. 6), $\xi^{(j)} = 2.553$ (except Figs. 3, 5, and 6), $\Omega = 1.3265$, $\epsilon = 0.596$, $d_0 = 0.1079$, and $N = 2$ (except Figs. 1-4 and Fig. 6). For simplicity, we define the sets $\bar{\alpha} = \{\alpha^{(j)}\}_{1 \leq j \leq N}$, $\bar{\beta} = \{\beta^{(j)}\}_{1 \leq j \leq N}$, $\bar{\xi} = \{\xi^{(j)}\}_{1 \leq j \leq N}$. The simulation was performed by generating 3×10^6 MRV-distributed random samples per each average SNR value.

Fig. 1 depicts the exact simulated and approximate PDF, computed using (1) and (2), respectively. One can ascertain that the two curves match tightly over the entire range of x and for several μ_1 values, showing the accuracy of (2). Importantly, the curves shift with μ_1 , and that the smaller μ_1 is, the more condensed are the random samples near to 0, leading to a higher peak of the PDF.

In Figs. 2 and 3, the MGF of the sum of N MRVs, given in (23)-(24), is plotted alongside its Monte Carlo simulation counterpart for both i.i.d and i.n.i.d cases. Again, it is clear that the two functions are matching for several values of $\mu_1^{(j)}$ and N . One can note evidently that the higher s is, the lower is the MGF. Additionally, one can see that, for a fixed value of s , the higher the average electrical SNR μ_1 , $\mu_1^{(j)}$ and N are, the lower the MGF value. Indeed, the greater these three parameters are, the higher the total average SNR $\bar{\gamma}_T$. Therefore, the more spread is the range of γ_T . Consequently, the MGF, defined as

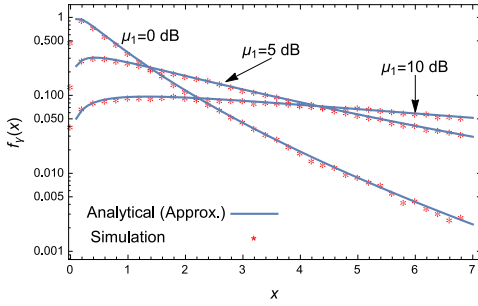


Fig. 1. Approximate PDF of MRV.

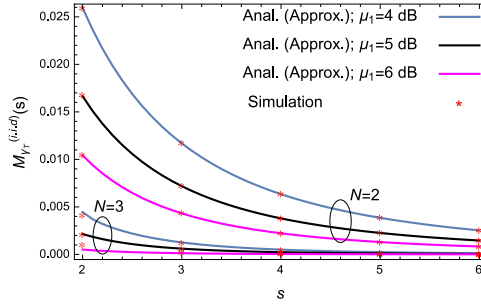


Fig. 2. MGF of the sum of i.i.d MRVs.

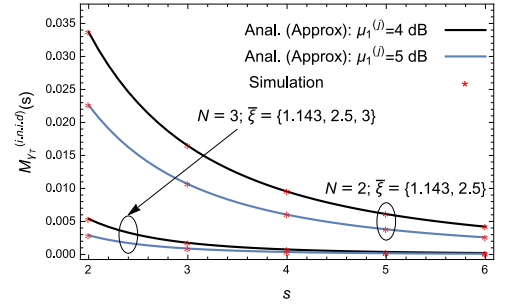
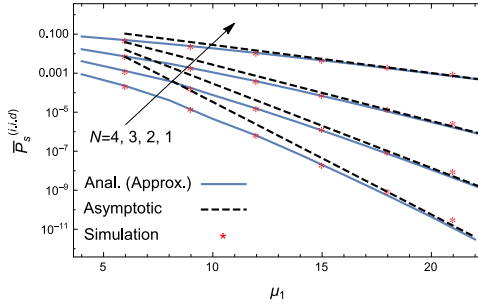
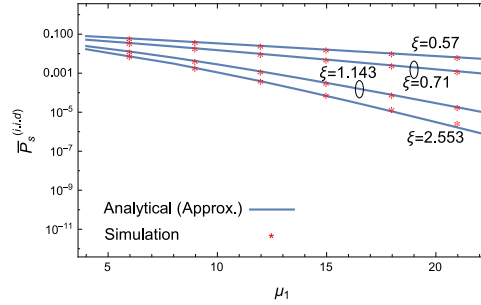
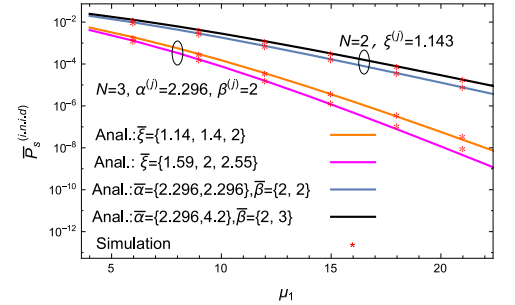


Fig. 3. MGF of the sum of i.n.i.d MRVs.

Fig. 4. ASER vs μ_1 for the i.i.d case.Fig. 5. ASER vs μ_1 for the i.i.d case with $N = 2$.Fig. 6. ASER vs μ_1 for the i.n.i.d case.

$M_{\gamma_T}(s) = \mathbb{E}[e^{-s\gamma_T}]$, decreases significantly. Furthermore, it is seen also that for higher N values (i.e., $N = 3$), the impact of μ_1 and $\mu_1^{(j)}$ is less significant on the MGF, particularly at higher values of s . This can be interpreted as the product $s\gamma_T$ is sufficiently higher to vanish the exponential term.

Fig. 4 highlights the ASER versus μ_1 of an N -branch MRC WCS, subject to i.i.d Málaga- \mathcal{M} fading with PEI, as given in (32), alongside its asymptotic result in (37). The ASER is plotted for BPSK modulation for various N values. It is evident that the analytical curves are tightly close to the Monte Carlo simulation ones, particularly for SNR values below 20 dB. Additionally, the greater μ_1 and N are, the enhanced is the overall system's ASER performance.

Fig. 5 depicts the ASER for the i.i.d fading case with $N = 2$ and several values of ξ . It can be noticed that the higher the ξ value, the lesser is the PEI effect, leading to an enhancement of the system's performance.

Fig. 6 shows the ASER versus $\mu_1 = \mu_1^{(j)}$ for the i.n.i.d scenario, given in (33), for various $\alpha^{(j)}$, $\beta^{(j)}$, and $\xi^{(j)}$ values. One can notice that the higher $\alpha^{(j)}$ and $\beta^{(j)}$ per branch, the overall system's ASER improves. Indeed, the higher these two parameters are, the lesser the turbulence effect. Again, the smaller $\xi^{(j)}$ per branch, the worse is the system's performance.

V. CONCLUSION

In this work, an accurate approximation for the statistics of the sum of MRVs was proposed. In particular, we proposed an approximation for the PDF of MRV, using the moments-based approach, by considering the first six moments, making it highly accurate. Next, the MGF of the sum of MRVs was retrieved, based on which, the respective ASER for MRC combining

scheme was derived in approximate and asymptotic forms, for both i.i.d and i.n.i.d fading scenarios. The assessed analysis showed that the proposed approximation yields a very close result to the exact simulation ones, for several values of the system's parameters. Additionally, the system's ASER performance is clearly impacted by the turbulence and PEI parameters. Lastly, the results showed that the achievable diversity order increases by increasing the number of the receiver's branches.

APPENDIX A: PROOF OF PROPOSITION 1

The moment-based approximation approach is opted in this work to retrieve an approximate RV $\hat{\gamma}$ for γ . It is worth noting that the greater the number of satisfied equations $\mathbb{E}[\hat{\gamma}^i] = \mathbb{E}[\gamma^i]$ ($0 \leq i \leq K-1$), the tighter is such an approximation. Owing to this fact, we choose $K = 6$ instead of $K = 5$ opted in [9]. In a similar manner to the last-mentioned work, $\hat{\gamma}$ is also considered in this work an H -distribution with K parameters $\{a_i\}_{1 \leq i \leq K}$, among them a_1 and a_2 are the scale factors of the PDF and x , respectively, as shown in (2). Moreover, the remaining ones are split between the integrand terms of the corresponding Mellin-Barnes integral, so as to reduce, relying on [12, Eq. (8.331.1)], the complexity of the following system of linear equations, obtained with the aid of the Mellin transform [13, Eq. (2.9)]

$$\mu_i = a_1 a_2^{i+1} \frac{\Gamma(a_5 + i + 1) \Gamma(a_6 + i + 1)}{\Gamma(a_3 + i + 1) \Gamma(a_4 + i + 1)}; 0 \leq i \leq K-1. \quad (43)$$

To this end, by considering that the moment of order $i = 0$ equals unity (i.e. $\mu_0 = 1$), (3) can be reached. Additionally, using [12, Eq. (8.331.1)], we get

$$\mathcal{L}_i - 2\mathcal{L}_{i-1} + \mathcal{L}_{i-2} = 2a_2; i \geq 3. \quad (44)$$

Thus, (4) can be readily obtained by setting $i = 4$ in (44). On the other hand, by putting i equal to 3 and 4 into (44), two equations are obtained. To this end, by making equality between the left hand-sides of the two obtained equations, alongside some algebraic manipulations, (5) is obtained. Analogously, by substituting $i = 4$ and 5 in (44), and making equality between the left hand-sides of the two obtained equations, one obtains (45), as shown at the bottom of the page.

Now, by plugging (5) into (45) and performing some algebraic operations, it yields (6). Moreover, we have the two following identities

$$\begin{cases} a_5 + a_6 + 2i + 1 = \frac{\mathcal{L}_{i+1} - \mathcal{L}_i}{a_2} \\ (a_5 + 1)(a_6 + 1) = \frac{\mathcal{L}_1}{a_2} \end{cases} . \quad (46)$$

By setting $i = 1$ in (46), a_5 and a_6 are attained as shown in (7) and (8), respectively.

REFERENCES

- [1] I. S. Ansari, F. Yilmaz, and M.-S. Alouini, "Performance analysis of free-space optical links over Málaga- \mathcal{M} turbulence channels with pointing errors," *IEEE Trans. Wireless Commun.*, vol. 15, no. 1, pp. 91–102, Jan. 2016.
- [2] A. Jurado-Navas, J. M. Garrido-Balsells, J. F. Paris, and A. Puerta-Notario, "A unifying statistical model for atmospheric optical scintillation," *Numerical Simulations of Physical and Engineering Processes*, J. Awrejcewicz, Ed., *Intech*, ch.8., pp. 181–206, Sep. 2011.
- [3] R. Boluda-Ruiz, A. García-Zambrana, B. Castillo-Vázquez, and C. Castillo-Vázquez, "On the capacity of MISO FSO systems over gamma-gamma and misalignment fading channels," *OSA Optics Express J.*, vol. 23, no. 17, pp. 22 371–22 385, Aug. 2015.
- [4] J. Ma, K. Li, L. Tan, S. Yu, and Y. Cao, "Performance analysis of satellite-to-ground downlink coherent optical communications with spatial diversity over Gamma-Gamma atmospheric turbulence," *OSA J. of Applied Optics*, vol. 54, pp. 7575–7585, Sep. 2015.
- [5] A. A. Ibrahim and T. Gucluoglu, "Performance analysis of maximum ratio transmission based FSO link over Málaga turbulence channel," *Optics Commun. J.*, vol. 450, no. 1, pp. 341–346, Nov. 2019.
- [6] M. Arti, "Product of squared SR random variables: Application to satellite communication," *IEEE Trans. on Aerospace and Elect. Systems*, vol. 56, no. 1, pp. 486–496, Feb. 2020.
- [7] S. Hazra and A. M. K., "Distribution of the product of squared correlated shadowed Rician random variables," in *2020 7th Int. Conf. on Signal Proc. and Integrated Networks (SPIN)*, 2020, pp. 409–413.
- [8] J. Ding, S. Yu, Y. Fu, J. Ma, and L. Tan, "New approximate and asymptotic closed-form expressions for the outage probability and the average BER of MIMO-FSO system with MRC diversity technique over Gamma-Gamma fading channels with generalized pointing errors," *Optics Commun. J.*, vol. 456, pp. 1–8, Feb. 2020.
- [9] F. El Bouanani and D. B. da Costa, "Accurate closed-form approximations for the sum of correlated Weibull random variables," *IEEE Wireless Commun. Lett.*, vol. 7, no. 4, pp. 498–501, Jan. 2018.
- [10] A. A. Kilbas and M. Saigo, *H-Transforms: Theory and Applications*. Boca Raton, Florida, US: CRC Press, 2004.
- [11] E. Illi, F. El Bouanani, and F. Ayoub, "A performance study of a hybrid 5G RF/FSO transmission system," in *Proc. of 2017 International Conference on Wireless Networks and Mobile Communications (WINCOM)*, 1-3 Nov. 2017, pp. 1–7.
- [12] I. S. Gradshteyn and I. M. Ryzhik, *Table of Integrals, Series, and Products: 7th Edition*. Burlington, MA: Elsevier, 2007.
- [13] A. Mathai, R. K. Saxena, and H. J. Haubol, *The H-Function Theory and Applications*. New York: Springer, 2010.

$$a_3 a_4 [\varphi_5 - 3\varphi_4 + 3\varphi_3 - \varphi_2] + (a_3 + a_4) [5\varphi_5 - 12\varphi_4 + 9\varphi_3 - 2\varphi_2] + 25\varphi_5 - 48\varphi_4 + 27\varphi_3 - 4\varphi_2 = 0. \quad (45)$$